ELSEVIER

Journal of Magnetism and Magnetic Materials 153 (1996) 302–310

journal of magnetism and magnetic materials

Magnetic viscosity of modified neodymium iron boron magnets with high coercivities

L. Jahn [a,*], R. Schumann [b], W. Rodewald [c]

[a] *Institute of Applied Physics, Dresden University of Technology, Mommsenstr. 13, D-01062 Dresden, Germany*
[b] *Institute of Theoretical Physics, Dresden University of Technology, Mommsenstr. 13, D-01062 Dresden, Germany*
[c] *Vacuumschmelze Hanau, PO Box 2253, D-63412 Hanau, Germany*

Received 18 October 1993; revised 17 July 1995

Abstract

In order to examine the long-term stability of novel Nd–Dy–Fe–Co–Mo–Al–B magnets with enhanced temperature stability, after-effect measurements have been carried out in an open circuit in the temperature range 20–230°C. In this temperature range the $\ln(t)$ law for the irreversible polarization losses is confirmed and the after-effect constant S and the fluctuation field S_v decrease monotonically with temperature for the sample annealed at an optimum. It can be proved that the open circuit measurements of S' and the irreversible susceptibility, $\chi'_{irr} = \chi'_{tot} - \chi'_{rev}$, should be corrected by the same the demagnetization coefficient N depending factor and thereafter that the S_v values can be derived directly by $S_v = S'_v = S'/\chi'_{irr}$. The determined room-temperature values of S_v between 8 and 11 kA m^{-1} are related to the coercivity approximately within the limits of a Barbier plot ($\log(S_v) = a \cdot \log(H_{cJ})$ with $a \approx 0.5$–1) and do not diminish the advantages of the low-temperature coefficient of the coercivity of the Nd–Dy–Fe–Co–Mo–Al–B magnets. The experimentally determined ratio S_v/T yields an activation volume V_c for the magnetization reversal corresponding to a critical diameter $d_c \approx 7$–14 nm, which is 1.5–2.5 times the Bloch wall thickness δ.

1. Introduction

Simultaneous additions of Co, Mo and Al to quasi-ternary $(Nd,Dy)_{15}Fe_{77}B_8$ effectively increase the coercivity H_{cJ} of sintered magnets [1,3,2].

The temperature coefficient of the coercivity is reduced in comparison with those of sintered $(Nd,Dy)_{15}Fe_{77}B_8$ magnets. This means $(Nd,Dy)_{14.1}(Fe,Co,Mo,Al)_{78}B_{7.9}$ magnets can be operated at temperatures up to 200°C. On the other hand, the long-term stability, particularly the irreversible polarization losses, is generally limited by the after-effect [4,7,5,8,17,14,12,19,27]. The thermal after-effect or magnetic viscosity has been investigated by many authors in the second quadrant of the hysteresis loops of various hard magnets [6,10,11,13,14] and of ternary Nd–Fe–B magnets [17,18,22–29]. The viscosity coefficient S is usually derived from the logarithmic time dependence of the isothermal polarization losses at a constant field in the second quadrant of the hysteresis loop. The fluctuation field, a temperature-dependent characteristic quantity of the material given by $S_v = S/(\chi_{irr})$; χ_{irr} denotes the irreversible susceptibility. According to the Barbier plot [9] S_v is expected to increase with increasing coercivity [19,11,27].

* Corresponding author. Fax: +49-351-463-3199; email: lj@padns1.phy.tu-dresden.de.

SSDI 0304-8853(95)00550-1

The aim of this paper is to examine the after-effect of the novel NdDyFeCoMoAlB magnets, in particular the correlation between S_v and H_{cJ} at temperatures up to 230°C. Because the measurements were performed in an open magnetic circuit, the effect of the load line of the magnet on the results has been calculated and checked experimentally.

The basic theoretical equations for the viscosity coefficient S are given in Refs. [13,16,31]. By the same procedure the irreversible susceptibility and the texture independence of S_v for two models of magnetization reversal have been derived [31,32].

2. Susceptibility and the open circuit

2.1. Theoretical background

Following the ideas of Néel [7] (see also Refs. [13,15,31]), the time- and field-dependent magnetization of the hard magnetic polycrystal is described by the distribution function of energy barriers (E_B) between the metastable and equilibrium states of saturated volume elements δV.

The averaged polarization of a polycrystal is

$$\frac{\bar{J}}{J_s} = \bar{m}(H,t) = \int_0^\infty \mathrm{d}E_B\, f(E_B)\, m(H,t)$$

$$= \int_0^\infty \mathrm{d}E_B [2p(t) - 1]\, f(E_B), \qquad (1)$$

where $p(t)$ is the probability of finding an initially opposite magnetized volume element in the metastable state at time t. Neglecting back-jumps, the probability is determined from

$$\mathrm{d}p/\mathrm{d}t = -\omega_{12}\, p, \qquad (2)$$

with the rate ω_{12} following an Arrhenius–Néel law, i.e. $\omega_{12} = \Gamma_0\, \mathrm{e}^{-E_B/kT}$. Γ_0 is the thermally activated attack frequency, which is generally of the order 10^{-9}–10^{-12} Hz [7]. $f(E_B)$ is the normalized barrier distribution function. The magnetic viscosity results from

$$S(H,t) = -\frac{\partial \bar{J}(H,t)}{\partial \ln t/s}$$

$$= 2J_s \int_0^\infty \mathrm{d}E_B\, f(E_B)\, \Gamma t\, \mathrm{e}^{-\Gamma t}. \qquad (3)$$

As shown in Refs. [15,31], the integral can be evaluated by a Taylor series expansion of the distribution function around the sharp maximum of $\Gamma t\, \mathrm{e}^{-\Gamma t}$, resulting in

$$\frac{S(H)}{J_s} = 2k_BT \sum_{n=0}^{\infty} C_n \frac{(-k_BT)^n}{n!} \frac{\mathrm{d}^n}{\mathrm{d}E_B^n} f(E_B)$$

$$\approx 2k_BT f(E_B)|_{E_{B,\max}}, \qquad (4)$$

with $E_{B,\max} = k_BT \ln \Gamma_0 t$ and

$$C_n = \int_0^\infty \mathrm{d}x \ln^n(x)\, \mathrm{e}^{-x}.$$

In most cases and in the following, the approximation of Eq. (4) adequately describes the experiments, and the well known expression for the time-dependent normalized polarization,

$$\bar{J}(H,t) = \bar{J}(H,t_s) - S \ln(t/t_s), \qquad (5)$$

allows us to fit S as well as the two parameters $\bar{J}(H,t_s)$ and t_s from the subsequent measured $\bar{J}(H,t)$ values.

2.2. Temperature dependence of the fluctuation field

As shown in Refs. [31] and following [13], from the same Eq. (1) the quantity χ_{irr} can be derived by differentiating $\bar{J}(H,t)$ with respect to H at a fixed time

$$\chi_{irr} = \frac{\partial \bar{J}(H,t)}{\mu_0 \partial H} = 2\frac{J_s}{\mu_0} \int_0^\infty \mathrm{d}E_B \frac{\partial f(E_B)}{\partial H} \mathrm{e}^{-\Gamma t}. \qquad (6)$$

Due to the implicit field dependence of $f(E_B)$ and taking into account that

$$\Gamma(0) = \Gamma_0, \quad \Gamma(\infty) = 0, \qquad (7a)$$

$$\frac{\partial \Gamma}{\partial E_B} = -\frac{\Gamma}{k_BT}, \quad f_H(\infty) = 0, \qquad (7b)$$

it follows after partial integration

$$\chi_{irr} = \frac{J_s}{\mu_0 k_BT} \frac{\mathrm{d}E_B}{\mathrm{d}H} \left(2\int_0^\infty \mathrm{d}E_B\, f(E_B)\, \Gamma t\, \mathrm{e}^{-\Gamma t} \right)$$

$$= \frac{S}{\mu_0 k_BT} \frac{\mathrm{d}E_B}{\mathrm{d}H}. \qquad (8)$$

Here a term was neglected, which is small due to

$\Gamma_0 \gg 1$. Usually the ratio of S and χ_{irr} is called the fluctuation field H_f [8] or S_v [7,11,14,24],

$$S_v = \frac{k_B T}{dE_B/dH} = \frac{k_B T}{V_c J_s}, \tag{9}$$

and S_v is discussed as a characteristic constant of the material. Its temperature dependence is determined by the competing behaviour of $k_B T$ and $[dE_B/dH](T)$ [17]. As shown in Ref. [13] for different models, the relation $dE_B/dH \sim V_c J_s$ holds, where V_c is the activation volume for the polarization reversal, which has to be determined from Eq. (9). According to different known mechanisms of reversal (e.g. coherent rotation, strong and weak domain wall pinning [13]) the fluctuation field may be field dependent.

At low temperatures the T-dependence of $\partial E/\partial H$ is weak [17], whereas at elevated temperatures $[\partial E/\partial H](T)$ dominates, resulting in a nearly linear decrease in $S_v(T)$ [18]. From Eq. (9) one gets the activation volume

$$V_c = \frac{k_B T}{S_v J_s}. \tag{10}$$

2.3. Influence of an open magnetic circuit

In the theory, all field- and time-dependent polarization changes correspond to the internal field H_{int}. If N is the demagnetizing coefficient, then the internal and external fields are related according to

$$H_{int} = H_{ext} - NJ/\mu_0. \tag{11}$$

If

$$\chi_{irr} = \frac{dJ_{irr}}{\mu_0 dH_{int}} \quad \text{and} \quad S = \left(\frac{\partial J}{\partial \ln t}\right)_{H_{int}} \tag{12}$$

are the susceptibility and the viscosity with respect to the internal field, and

$$\chi'_{irr} = \frac{dJ_{irr}}{\mu_0 dH_{ext}} \quad \text{and} \quad S' = \left(\frac{\partial J}{\partial \ln t}\right)_{H_{ext}}, \tag{13}$$

with respect to the external field, it follows from (11)

$$\chi_{irr} = \frac{\chi'_{irr}}{1 - N\chi'}, \tag{14}$$

$$S = \frac{S'}{1 - N\chi'}, \tag{15}$$

where χ' is the total susceptibility with respect to the external field. This agrees with Refs. [26,21] and disagrees with many authors [6,13,24] who used the reversible or averaged susceptibilities for the corrections on the internal field. Division of Eq. (15) by Eq. (14) yields

$$S_v = S'_v, \tag{16}$$

thus proving that the fluctuation field as the ratio of S and χ_{irr} is not affected by measurements in an open circuit.

Often the after-effect measurements in high-coercivity, well-textured rare earth magnets are performed in the field range near H_{cJ} only. If both $\chi_{irr} \approx$ const. and $\chi_{rev} \approx 0$ hold, the procedure in Refs. [10,19] becomes applicable, where the fluctuation field is obtained directly by the difference between the external field H_1, i.e. the constant field during irreversible polarization decrease, and H_2, corresponding to the same polarization value on the fast measured $J(H)$ curve.

3. Experiments

3.1. Sample preparation and magnetic measurements

Nd–Dy–Fe–B alloys with different dysprosium concentrations of 1 or 3 at% and a Nd–Dy–Fe–Co–Mo–Al–B alloy with a Dy concentration of 2.9 at%, a Co concentration of 5 at%, a Mo concentration of 4 at% and 0.5 at% Al were melted in a vacuum induction furnace from pure metals or a Fe–18 at% B master alloy, respectively (see Table 1).

The ingots were crushed and milled to powders with an average particle size of about 3 μm. The powders were aligned in magnetic field of 13.5 kA cm^{-1}, pressed isostatically with 200 MP and sintered at temperatures 1080–1150°C. Different isothermal annealings at temperatures 600–900°C were performed in order to optimize the coercive field strength.

After magnetizing the spherical, prismatic or cylindrical samples in pulse fields of about $H \approx 56$ kA cm^{-1} the isothermal $J(H)$ and $J(T)_H$- measurements in the second quadrant of the hysteresis loop were performed in air by means of a vibrating sample magnetometer (maximum field of 21 kA cm^{-1}).

Table 1
Compositions, annealing temperatures T_A and room-temperature characteristics of the investigated sintered magnets

Composition	Sample	T_A (°C)	Density (g cm^{-3})	$J(B=-\mu_0 H)$ (T)	H_{cJ} (kA cm^{-1})
$(Nd,Dy)_{14.1}Fe_{68.5}Co_5Mo_4Al_{0.5}B_{7.9}$	V1	750	7.6	1.02	19.2
$(Nd,Dy)_{14.1}Fe_{68.5}Co_5Mo_4Al_{0.5}B_{7.9}$	V2	850	7.6	0.99	8.4
$(Nd,Dy)_{14.1}Fe_{68.5}Co_5Mo_4Al_{0.5}B_{7.9}$	V3	630	7.6	0.99	18.8
$Nd_{12}Dy_3Fe_{77}B_8$	V4	630	7.4	1.12	20.0
$Nd_{14}Dy_1Fe_{77}B_8$	V6	630	7.6	1.29	12.4

Fig. 1 shows the measured demagnetization curve at room temperature for a prismatic sample V1 ($N \approx 0.25$) before (a) and after (b) the correction of the image effect. The two magnifications below, which correspond to the points 1 and 2 in the second quadrant, demonstrate the determination of χ'_{rev} after a time interval of approximately 10 min [24]. Within the limits of experimental accuracy, due to further creeping of the magnetization in the vicinity of H_{cJ}, the reversible susceptibility is found to be $\chi'_{rev} \approx 0$.

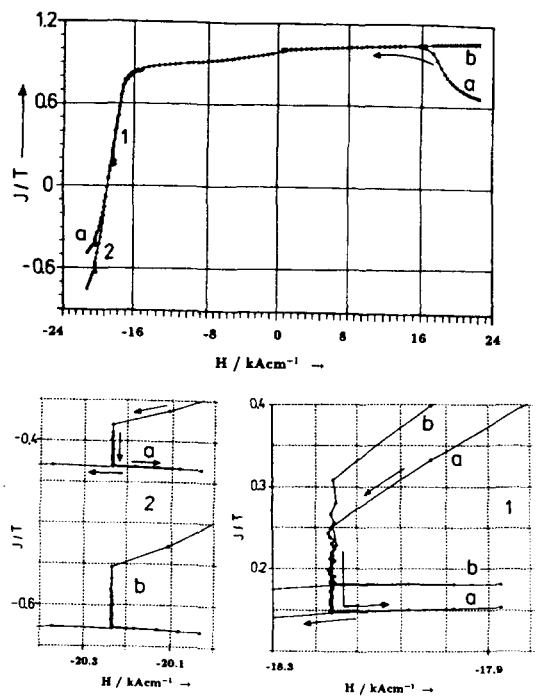

Fig. 1. Measured (a) and corrected (b) demagnetization curve $J(H)$ at room temperature, sample V1 (prism $N \approx 0.25$). Below: Magnifications of the regions 1 and 2 with reversible recoil loops. Time intervals between subsequent points amounts to 17 s.

Because the magnetic field was generated by means of an iron yoke, the measured magnetization decreases for fields above $H \approx 13.6$ kA cm^{-1} (curve a in Fig. 1). This systematic error, denoted as the image effect, depends on the sample shape. In order to correct it, we extrapolated that part of the magnetization curve that was measured between 4.8 and 12 kA m^{-1}, to higher values. While fitting, we take into account the given alignment of the sample, which for all well aligned samples ($B_r/J_s \approx 0.97$) leads to a straight line within the limits of experimental error. The ratio of the extrapolated (curve b in Fig. 1) and the measured polarization values (part a of Fig. 1) is the field- dependent image effect correction factor, which has been used separately for every sample in order to compensate for this effect in the second quadrant of the hysteresis loop (see Fig. 1).

In Eq. (5) the time (t and t_s) is related to the time $t=0$, at which the probability that each grain remains in the saturated state, yields $p(0)=1$ [15]. This time is different from the experimental time t_{exp}, because the point $t=0$ is not known exactly. The measurements of $J(t_{exp})$ start with $t_{exp}=0$ at the point t_s, and formula (5) becomes

$$J(t_{exp}) = J_1(t_s) - S' \cdot \ln\left(\frac{t_{exp}-t_s}{1\ \text{min}}\right)$$

$$= J_2(t_s) - S' \cdot \ln\left(\frac{t_{exp}-t_s}{1\ \text{s}}\right). \qquad (17)$$

For the determination of S' the parameters S', t_s and $J(t_s)$ have been fitted by means of standard fitting programs. S' is independent of the time scale, whereas the less important parameter $J(t_s)$ is influenced (e.g. $J_1(t_s) = J_2(t_s) + S' \ln(1/60)$). No deviations from the $\ln(t)$ law could be observed.

3.2. Experimental results

The field dependence of the after-effect constants S' near H_{cJ} for samples 1–3 are given in Fig. 2. The figure shows $\chi'(H)$ for sample V1 and the theoretically expected maximum near H_{cJ}, which is indicated by vertical arrows. However, we found the shape of $\chi'(H)$ to be much broader than that of $S'(H)$ in the vicinity of H_{cJ} for the anisotropic magnets. Therefore the field dependencies of $S_v(H)$ and $S'(H)$ are similar. That is why we used the maximum values of S' and S_v in order to determine the temperature dependence up to 230°C. In Figs. 3–5 we show plots of the temperature dependence of the measured H_{cJ} and S', as well as $S_v = S'/\chi'_{irr}$. Especially in the range 100–200°C fairly linear decreases in the three quantities were found. The corresponding temperature coefficients (α) for a linear fit, e.g. $H_{cJ}(T) = H_{cJ}(0)(1 - \alpha_{(H_{cJ})}\Delta T)$, are listed in Table 2.

The third column of Table 2 shows the minimum of $\alpha_{(H_{cJ})}$ for sample V1 which, together with high absolute H_{cJ} values, demonstrates the technical importance of this magnet annealed at optimum [3,1]. The similar temperature coefficients of S_v and H_{cJ} of all investigated magnets demonstrate their strong correlation, which is obvious in the Barbier plot [9]. The double logarithmic diagram for the related S_v and H_{cJ} values of the five samples, obtained at different temperatures, are compiled in Fig. 6. However, from the linear regression

$$\log(S_v) = a \cdot \log(H_{cJ}) + b, \tag{18}$$

two different slopes $a_1 \approx 0.5$ or $a_2 \approx 1.0$ at room temperature or 200°C, respectively, result.

4. Discussion

For very short and very long measuring times (e.g. [14]) and for small distribution functions of the particle coercivities [29] and energy barriers a systematic deviation from the ln(t) law is to be expected. In the experiments with time intervals between 1 and 30 min the ln(t) law holds.

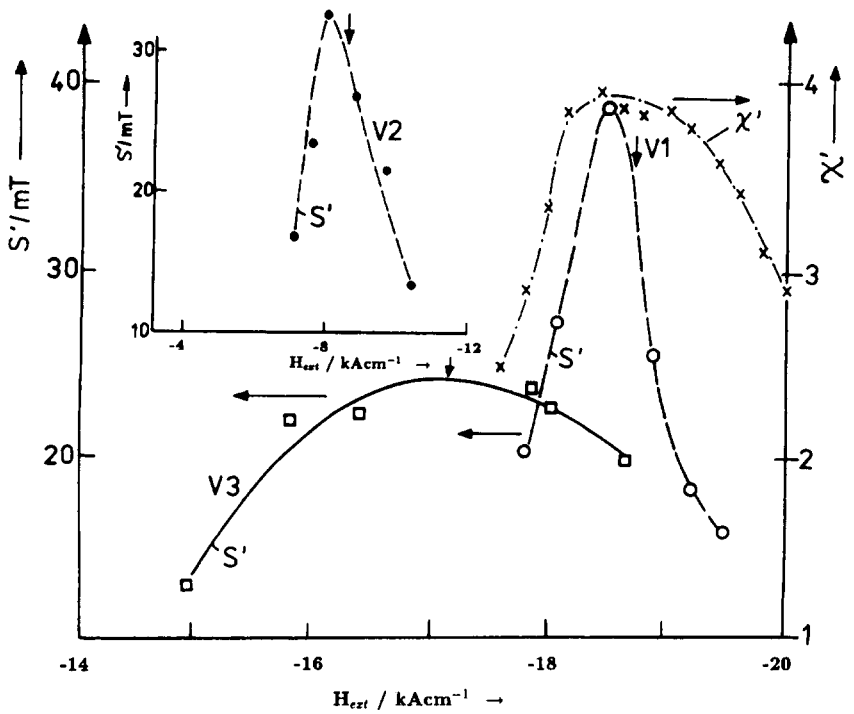

Fig. 2. Field dependence of the after-effect constant S' for external fields $0.9H_{cJ} < H_{ex} < 1.1H_{cJ}$ at room temperature for samples V1, V2 and V3; $\chi'(H)$ for sample V1; vertical arrows indicate the coercivity.

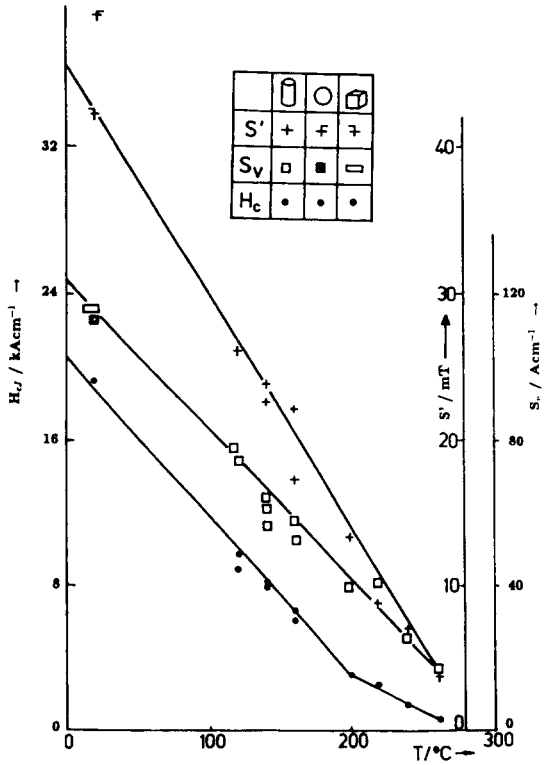

Fig. 3. Temperature dependence of the coercivity H_{cJ}, maximum after-effect constant S' and fluctuation field S_v for the $Nd_{11.2}Dy_{2.9}Fe_{68.5}Co_5Mo_4Al_{0.5}B_{7.9}$ magnet, annealed at 750°C for 1 h.

A comparison of the results of the S' and S_v values given in the literature is difficult due to the many different experimental and theoretical procedures. But the determined absolute room-temperature values of S_v between 80 and 110 A cm^{-1} agree fairly well with those given in Refs. [17,27,24] for Nd–Fe–B magnets.

For the after-effect measurements in an open magnetic circuit it was proved that for the shearing correction from the used external to the internal field only the total susceptibility (and not any mixture, e.g. Refs. [20,13]) determines the viscosity coefficient as well as the irreversible susceptibility. It should be emphasized that S_v does not depend on the demagnetizing coefficient N, i.e.

$$S_v = \frac{S}{\chi_{irr}} = S'_v = \frac{S'}{\chi'_{irr}}.$$

Since the N values of our differently shaped samples did not differ significantly, this could be proved only for demagnetization coefficients in the range $0.25 \leq N \leq 0.35$. The remarkable difference in S' for the different samples of V2 at room temperature (Fig. 4) are partly due to differences in χ_{irr}.

Disregarding possible higher S_v values in fields far beyond the coercivity [26] our investigations focused on the field region near the coercivity. Following our result that $\chi'_{rev} \approx 0$ holds in the vicinity of $H \approx (1 \pm 0.1)H_{cJ}$, the irreversible susceptibility $\chi'_{irr} \approx \chi' = \chi_{tot}$ is given by the field derivative $dJ/\mu_0 dH$ of the demagnetization curve (cf. Figs. 1 and 2). Although from the theoretical point of view a very fast measurement of $\chi_{tot} = dJ/\mu_0 dH$ is required, our static measurements were carried out with time intervals of (5...17) s between subsequent points. Nevertheless the maximum values of χ'_{irr} are located at approximately $1/N$. In contrast with the results given in Ref. [17] for our well aligned magnets with $B_r/I_s = 0.97$ [33,34], the field dependence of χ' shows a broader shape than that of S' in the coercivity region (in agreement with Ref. [35]), resulting in a field dependence of S_v near H_{cJ}. The

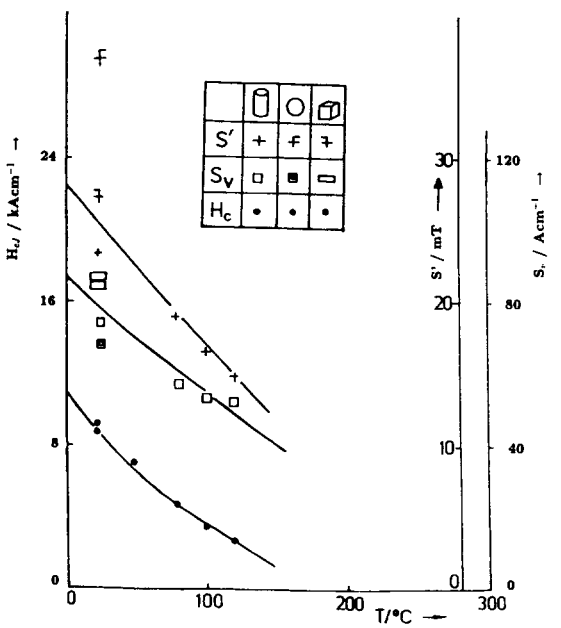

Fig. 4. Temperature dependence of the coercivity H_{cJ}, maximum after-effect constant S' and fluctuation field S_v for the $Nd_{11.2}Dy_{2.9}Fe_{68.5}Co_5Mo_4Al_{0.5}B_{7.9}$ magnet, annealed at 850°C for 1 h.

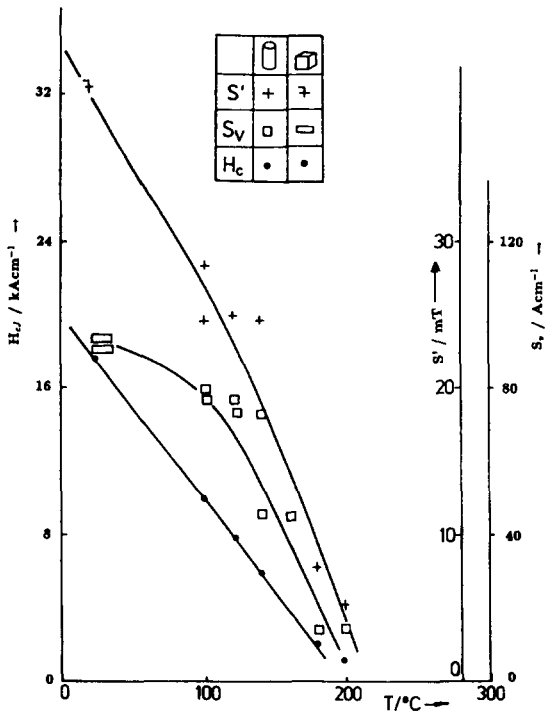

Fig. 5. Temperature dependence of the coercivity H_{cJ}, maximum after-effect constant S' and fluctuation field S_v for the $Nd_{11.2}Dy_{2.9}Fe_{68.5}Co_5Mo_4Al_{0.5}B_{7.9}$ magnet, annealed at 630°C for 1 h.

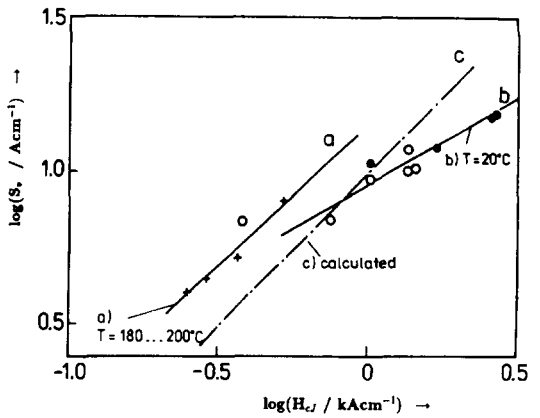

Fig. 6. Barbier plots, $\log(S_v) = a \cdot \log(H_{cJ})$. (a) 180–200°C (crosses, without V2); (b) 20°C (full circles), 100°C (empty circles); (c) theoretically expected [22].

very high S_v values may be due to large magnetostatic interaction (avalanche) effects of the magnetization reversal near the coercivity [38,39].

Far above the $S_v(T)$ maximum reported for lower temperatures in the ternary system [17] in the investigated temperature range (20–30°C), the fluctuation field $S_v(T)$ shows a monotonous decrease. This monotonous decrease in $S'(T)$ and $S_v(T)$ has to be

Table 2
Measured values of H_{cJ}, S' and S_v at room temperature and the temperature coefficients $\alpha_{(HcJ)}$, $\alpha_{(S')}$ and $\alpha_{(S_v)}$

Sample	H_{cJ} (20°C) (kA cm^{-1})	$\alpha_{(HcJ)}$ (K^{-1})	S' (20°C) (mT)	$\alpha_{(S')}$ (K^{-1})	S_v (20°C) (A cm^{-1})	$\alpha_{(S_v)}$ (K^{-1})
V1	19.2	0.0043	41	0.0035	110	0.0033
V2	8.4	0.0067	26	0.0038	80	0.0035
V3	18.8	0.0050	40	–	95	
V4	20.	0.0048	46	0.0032	120	0.0036
V6	12.4	0.0055	32	0.0043	90	0.0042

Table 3
Estimation of the critical volume V_c, the corresponding diameter d_c and a comparison with the wall thickness δ; A = exchange constant

Sample	T (K)	J_s (T)	S_v (A cm^{-1})	V_c (10^{-27} m^3)	d_c (nm)	$A(T)$ (10^{-11} J m^{-1})	δ (nm)
V1	293	1.0	110	355	7	0.6	3.2
V1	473	0.8	50	2050	13	0.4	4.5
V2	293	1.0	100	510	8		
V2	473	0.8	30	2700	14		

discussed in terms of the predominant influence of dE_B/dH in Eq. (9) [17] above room temperature.

For the five magnets with different compositions and heat treatments the double-logarithmic Barbier plots of the corresponding isothermal H_{cJ} and S_v values show at higher temperatures ($\sim 200°C$) the theoretical expected slope $a_1 = 1$ [27], whereas at room temperature the slope is only $a_2 \approx 0.5$.

Finally, from the determined temperature dependence of S_v the activation volume for the magnetization reversal has been estimated. From Eq. (10) the activation volume and the corresponding diameter d_c were calculated from $d_c = (V_c)^{1/3}$ (cf. Table 3). This should be compared with the Bloch wall thickness. Whereas for (Nd,Dy)FeCoMoAlB sintered magnets only the temperature-dependent Bloch wall energy $\gamma(T)$ is given in Ref. [30], the wall thickness has been estimated by

$$\delta \approx \pi\sqrt{A(T)/(K_1(T)(1+K_2/K_1))}\,.$$

The exchange constant A has been taken from Ref. [36] for ternary Nd–Fe–B magnets and the anisotropy constants $K_1(T)$, $K_2(T)$ for magnets with the hard magnetic $Nd_{0.9}Dy_{0.1}Fe_{14}B$ compound ware taken from Ref. [37].

These d_c values are 1.5–2.5 times the Bloch wall thickness δ for ternary Nd–Fe–B crystals, and show the same tendency with increasing temperature as expected following Eq. (10) and Ref. [17]. This is a week argument for the qualitative validity of Eq. (10).

As a concluding remark it should be pointed out that the improved temperature stability of the novel Nd–Dy–Fe–Co–Mo–Al–B magnets due to the high coercivity and the lower temperature coefficient of H_c is not diminished by any anomalously high thermal after-effect.

Acknowledgements

The authors wishes to thank Dr E. Adler and Dr D. Eckert for stimulating discussions, Mrs A. Franke and Mr M. Starke for technical assistance and the Bundesministerium für Forschung und Technologie, Germany, for financial support (contract No. 03M5007C9).

References

[1] W. Rodewald and B. Wall, J. Magn. Magn. Mater. 101 (1991) 338 40.
[2] P. Tenaud, F. Vial and M. Sagawa, IEEE Trans. Magn. 26 (1990) 1930.
[3] S. Hirosawa, H. Tomizawa, S. Mino and A. Hamamura, IEEE Trans. Magn. 26 (1990) 1960.
[4] R. Street and J.C. Woolley, Proc. Phys. Soc. A 62 (1949) 562.
[5] R. Street, R.K. Day and J.B. Dunlop, in: Proc. 5th Int. Symp. on Magnetic Anisotropy and Coercivity in RE–TM Alloys (1987) p. 329.
[6] J. Shi, O. Yamada, H. Maruyama, M. Sagawa and S. Hirosawa, IEEE Trans. Magn. 23 (1987) 3122.
[7] L. Néel, J. Phys. Radium 12 (1951) 339.
[8] E.P. Wohlfarth, J. Phys. F 14 (1984) L155.
[9] J.C. Barbier, Ann. Physique (Paris) 9 (1954) 84.
[10] W. Rodewald, 4th Symp. on Magnetic Anisotropy and Coercivity in RE–TM Alloys, Dayton, OH, 1985, paper X-3.
[11] E. Adler, Ber. AG Magnetismus 1 (1982) 41.
[12] E. Adler and H.-J. Marik, in: Proc. 5th Int. Workshop on RE Magnets and their Applications, Roanoke, 1981, 335 (Book University of Dayton, KI-365), paper VII-3.
[13] P. Gaunt, J. Appl. Phys. 59 (1986) 4129.
[14] A. Gladun and D. Eckert, J. Magn. Magn. Mater. 73 (1988) 136.
[15] D.V. Berkov, J. Magn. Magn. Mater. 111 (1992) 327.
[16] D.V. Berkov, J. Magn. Magn. Mater. 123 (1992).
[17] D. Givord, A. Lienhard, P. Tenaud and T. Viadieu, J. Magn. Magn. Mater. 67 (1987) L281.
[18] D. Givord, P. Tenaud and T. Viadieu, J. Appl. Phys. 61 (1987) 3454.
[19] W. Fernengel and E. Adler, in: Proc. 10th Int. Workshop on RE Magnets and their Applications, Kyoto, 1989.
[20] E.W. Singleton and G.C. Hadjipanayis, 6th Int. Symp. on RE–T Metals, Pittsburgh, 1990, paper 2.6.
[21] A.J. Schwarz and W.A. Soffa, IEEE Trans. Magn. 26 (1990) 1816.
[22] Liu Jinfang, Pan Shuming, Luo Helie, Hou Denglu and Nie Xianfu, J. Phys. D: Appl. Phys. 24 (1991) 384.
[23] H. Nishio, Jpn. J. Appl. Phys. 27 (1988) 136.
[24] H. Nishio, IEEE Trans. J. Magn. Jpn. 5 (1990) 374.
[25] R. Skomski and V. Christoph, Phys. Stat. Solidi (b) 156 (1989) K149.
[26] G.J. Tomka, P.R. Bissell, K. O'Grady and R.W. Chantrell, IEEE Trans. Magn. 26 (1990) 2655.
[27] J. Liu, H. Luo and S. Pan, J. Appl. Phys. 69 (1991) 5557.
[28] J. Liu, S. Pan, H. Luo, D. Hou and X. Nie, J. Phys. D 24 (1991) 384.
[29] M. El-Hilo, K. O'Grady and R.W. Chantrell, J. Magn. Magn. Mater. 109 (1992) L164.
[30] K. Bockmann, PhD Thesis, Universität Nürnberg, 1994.
[31] R. Schumann and L. Jahn, J. Magn. Magn. Mater. 149 (1995) 318.
[32] R. Schumann, J. Magn. Magn. Mater. 150 (1995) 349.

[33] L. Jahn, W. Rodewald, V. Christoph and R. Scholl, J. Magn. Magn. Mater. 118 (1993) 33.
[34] L. Jahn, V. Christoph, D. Eckert, R. Schumann, K.-H. Müller and R. Scholl, in: Proc. 2nd Int. Symp. on Phys. Magn. Mater. (ISPMM 92), Beijing, July 1992, p. 42.
[35] D. Eckert, K.-H. Müller, P.A.P. Wendhausen and M. Wolf, Conf. Proc. EMMA 1993, B-O-02.
[36] M.K. Neudecker, Thesis, UNI Nürnberg–Erlangen, 1990.
[37] S. Hock, Thesis, MPI Stuttgart, 1988.
[38] U. Heinecke und O. Henkel, Conf. Struktur und Eigenschaften magnetischer Festkörper, Leipzig, 1967.
[39] R. Blank, W. Rodewald and W. Schleede, in: Proc. 10th Int. Workshop on RE Magnets and their Applications, Kyoto, 1989, p. 353.